

# 28 GHz Switched Beam Vivaldi Antenna System for V2V Communication in 5G Applications

Allam M. AMEEN<sup>1,2</sup>, Mohamed I. AHMED<sup>2</sup>, Hala ELSADEK<sup>2</sup>, Wagdy R. ANIS<sup>1</sup>

<sup>1</sup> Electronics and Electrical Communication Eng. Dept., Faculty of Engineering, Ain Shams University, 11566 Cairo, Egypt  
<sup>2</sup> Microstrip Dept., Electronics Research Institute, New Nozha, 11843 Cairo, Egypt

allamameen@eri.sci.eg, {miahmed, helsadek}@eri.sci.eg, wagdyanis51@yahoo.com

Submitted October 5, 2021 / Accepted January 10, 2022

**Abstract.** A 28 GHz switched beam Vivaldi antenna system consisting of 4 Vivaldi antennas for V2V communication is presented. The proposed design is realized on a substrate material of “Rogers 5880” with  $\epsilon_r = 2.2$ ,  $\tan\delta = 0.002$  and 0.508 mm substrate thickness. The antenna is designed to operate at a center frequency of 28 GHz with operating bandwidth of 1.463 GHz (5.23%). An overall realized gain of 9.78 dBi is achieved at the intended center frequency. The proposed antenna is designed and simulated. It is also fabricated using photolithography techniques and measured using R&S vector network analyzer. Good agreement is obtained between both simulated and measured results.

## Keywords

Circular array antenna, switched beam antenna, Vehicle-to-Vehicle (V2V) communication, Vivaldi antenna, ITS, 5G applications

## 1. Introduction

Vehicle-to-Vehicle (V2V) communication systems have rapidly developed and applied to enable efficient road transport and more safety. Intelligence transportation system (ITS) is built depending on Dedicated Short Range Communication (DSRC) technology which presents a high reliability and a fast data transmission [1–4]. This system improves the road safety to avoid car accidents and reduce the traffic jam by sending all the information about the road to the drivers to make decisions. There are four classifications of V2X wireless communications, vehicle-to-vehicle (V2V), vehicle-to-personal (V2P), vehicle-to-infrastructure (V2I), and vehicle-to-network (V2N) [5–8]. A low-profile monopolar was introduced and two antenna designs were presented: a low-profile and a flush-mounted [9]. Both two antennas were surrounded by a thin plastic radome. Four elements-monocone broadband antenna for V2X wireless communication is introduced [10]. Three antennas were proposed and discussed in the cavity to offer a significantly room for antennas and radio frequency [11]. A low-profile wideband monopolar antenna size is reduced by adding four tapered slots which make it applicable for vehicles and

helmets [12]. Three antenna arrays consisting of 16 patches in each array were developed to operate at 61 GHz [13].

There are many techniques for beam switching that can be used to reconfigure the radiated beams [14], [15]. Some of them are traditional such as digital beamforming [16], butler matrix [17], and array antennas [18–21]. Array of an antipodal Vivaldi antenna (AVA) with gradual corrugated edges (GCEs) and triangular metal directors (MDs) is presented and discussed in [18]. Two orthogonally polarized Vivaldi MIMO antennas operating at 28/38 GHz for base station are introduced in [22]. Narrow bandwidth, bulky structure and complicated beam forming networks are disadvantages of these methods at microwave frequencies. Another method to satisfy the beam switching configuration is by using PIN diodes which operated by DC controlled circuit [23–26]. In [23], RF switch controlled by a microcontroller to feed a 2×2 array antenna is introduced.

In this paper, four switched beam Vivaldi antennas with single port are designed, simulated and fabricated for V2V wireless communication system. The proposed antenna provides a full 360° coverage area with high gain and large distance compared with omnidirectional one. The antenna is designed to operate at frequency of 28 GHz for mm-wave and 5G applications.

## 2. Proposed Antenna Design

Four symmetric microstrip Vivaldi antennas placed at different directions with angle 90° between each two antennas to cover the full 360° area. Five PIN-diodes are used to connect the single port of the structure to each antenna. A controlled circuit is applied to switch the PIN-diodes ON/OFF states. Details of the single patch antenna and the overall structure are described below.

### 2.1 Single Microstrip Vivaldi Antenna

Figure 1 shows the design of the proposed Vivaldi antenna and its structure. The structure of the proposed antenna is realized by subtraction an elliptical shape from the rectangular patch antenna on each side. The antenna is placed on a substrate of type “Roger 5880” with  $\epsilon_r = 2.2$ ,

$\tan\delta = 0.002$  and  $0.508$  mm thickness. The overall antenna size for a single patch is  $L_{sub} = 32.25$  mm and  $W_{sub} = 16$  mm. Table 1 shows the dimensions of the structure in mm. The dimensions of  $R_i$ ,  $R_{out}$  and  $R_g$  represent an inner radius of the patch, an outer radius of the patch and a minor radius of an ellipse cut in the ground respectively. Figure 2 shows the return loss of the single patch antenna.

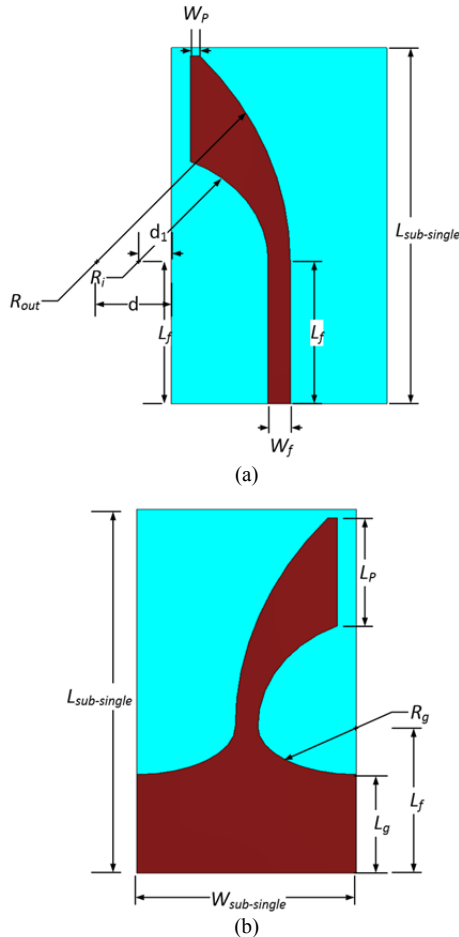


Fig. 1. The design of the proposed Vivaldi antenna element and its structure: (a) front view, and (b) back view.

Parameter	Length [mm]	Parameter	Length [mm]
$L_{sub-single}$	32.25	$W_{sub-single}$	16
$L_p$	9.581	$W_p$	0.705
$L_f$	13	$W_f$	1.65
$L_g$	8.75	$R_g$	4.25
$R_i$	9.775	$R_{out}$	28.825
$d$	20	$d_1$	4

Tab. 1. The dimensions of the proposed single antenna element in the designed structure.

A parametric study is obtained for each dimension individually while the other parameters are constant. Figure 3a discusses the effect of changing the length of  $L_p$  which tends to shift the resonance frequency and change the value of return loss ( $S_{11}$ ). Increasing of  $L_p$  tends to increase the resonance frequency and increase the return loss

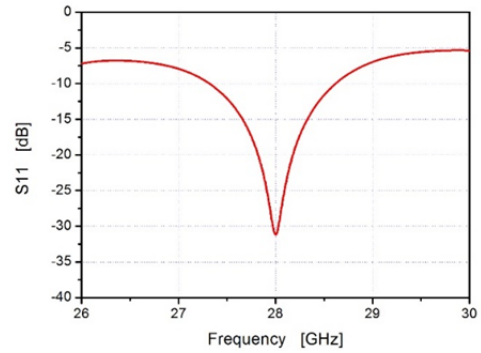


Fig. 2. The reflection coefficient of the single patch antenna.

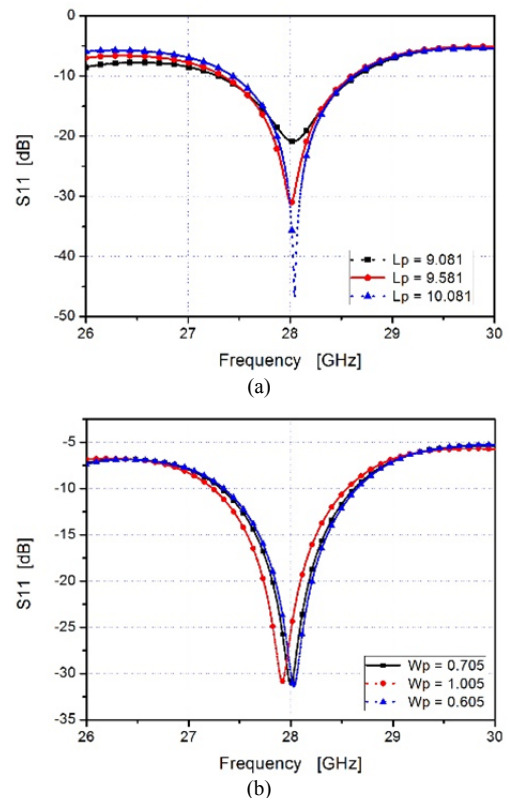


Fig. 3. A parametric study of increasing and decreasing of (a) the length  $L_p$ , (b) the width  $W_p$ .

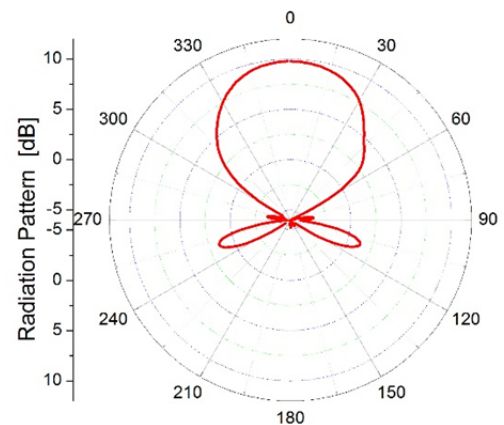


Fig. 4. The simulated radiation pattern of the single patch Vivaldi antenna.

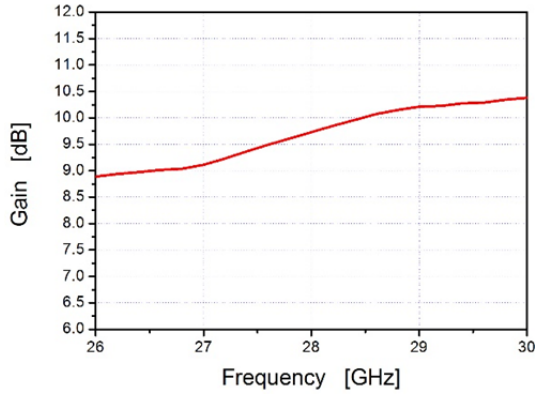


Fig. 5. The overall antenna gain for the single patch antenna.

while the gain decreases. In Fig. 3b, increasing of  $W_p$  tends to decrease the resonance frequency while the return loss ( $S_{11}$ ) approximately remains the same. Elaborating results of all parametric studies, it is easy to choose the proper the dimensions that achieve the resonant frequency at 28 GHz based on the required specifications and application. Figure 4 shows the radiation pattern of the proposed antenna at the resonant frequency. In Fig. 5, the overall antenna gain for the single patch element is presented.

### 2.2 Proposed Complete Structure

The designed structure consists of four elements of the Vivaldi antenna designed. The four elements are constructed to cover the overall area by making the angle between any two elements equal 90 degrees so the overall coverage angle will be 360 degrees as shown in Fig. 6. The main benefit to use this structure instead of an omnidirectional antenna is the high gain and long distance that the signal can travel comparing with the omnidirectional antenna. One microstrip feedline is used to feed the four elements. PIN diodes controlled by switching circuits are used to select the radiated antenna sequentially to transmit and receive the signals in all directions. PIN diodes offer a very good linearity and are applied for high power applications at microwave frequencies. An AlGaAs PIN diode of type “MA4AGBLP912” with a small on resistance, low capacitance and significant fast switching speed is applied. The proposed structure is shown in Fig. 6. The relationship between the switched RF diodes and the four radiators antenna structure is tabulated in Tab. 2. The shape of feed-line is different in each case so a parametric study for the shape of the feedline is presented in Fig. 7. A groove between each two elements is used to enhance the system operation and improve the return loss.

State	Switched Diodes					Radiator
	D1	D2	D3	D4	D5	
1	ON	OFF	OFF	OFF	OFF	Antenna 1
2	OFF	OFF	ON	OFF	ON	Antenna 2
3	OFF	OFF	ON	ON	OFF	Antenna 3
4	OFF	ON	OFF	OFF	OFF	Antenna 4

Tab. 2. Four configurations of the proposed antenna using switched RF diodes.

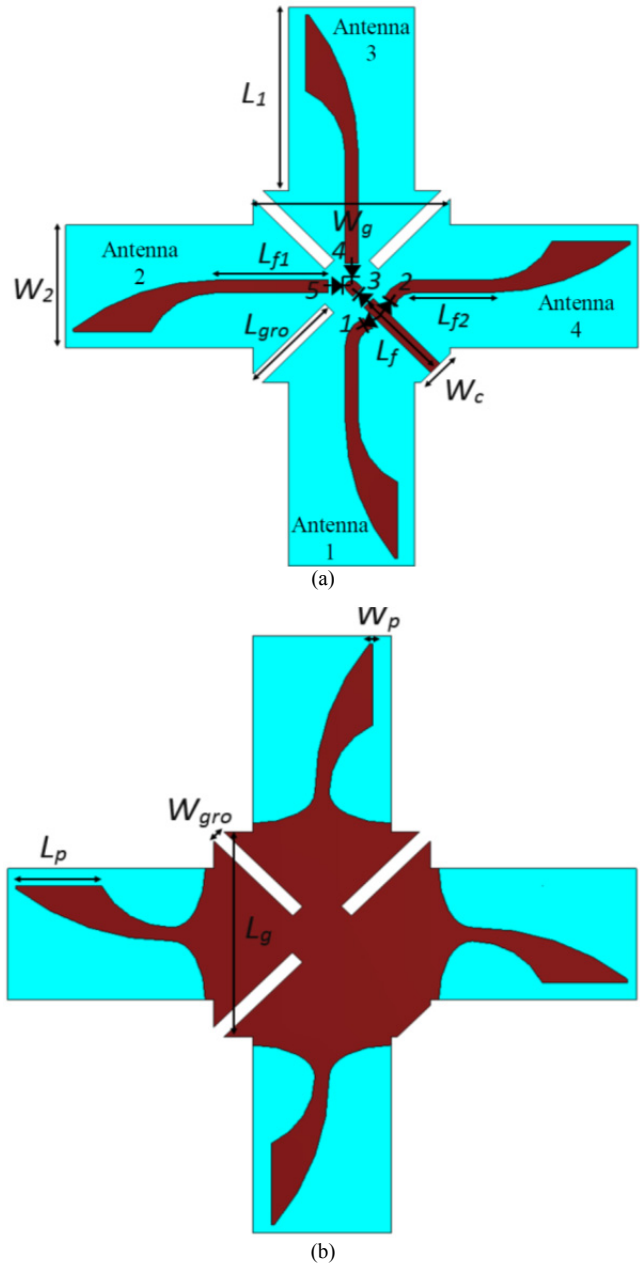


Fig. 6. The complete proposed structure with 4 elements.

Parameter	Length [mm]	Parameter	Length [mm]
$L_1$	23.85	$W_1$	16
$L_p$	9.882	$W_p$	0.39
$L_f$	12	$W_f$	1.65
$L_{r1}$	14.35	$L_{r2}$	9.60
$L_g$	25	$W_g$	25
$L_{gro}$	12.85	$W_{gro}$	1.65
$R_g$	4.25	$W_c$	5.355
$R_i$	9.775	$R_{out}$	28.825

Tab. 3. The dimensions of the overall proposed antenna structure.

Table 3 shows additional dimensions for the proposed structure. In Fig. 8, the return loss ( $S_{11}$ ) of the four ele-

ments is shown. Figure 9 shows the radiation pattern of the proposed structure. In this figure, for example, the diodes D3 and D5 are ON and D1, D2 and D4 are OFF, then the antenna 2 will operate and the radiation will be in  $-90^\circ$  direction. The diodes D3 and D4 are ON and D1, D2 and D5 are OFF, then the antenna 3 will operate and the radiation will be in  $0^\circ$  direction and so on. The overall gain over the frequency range of operation for the full structure is studied.

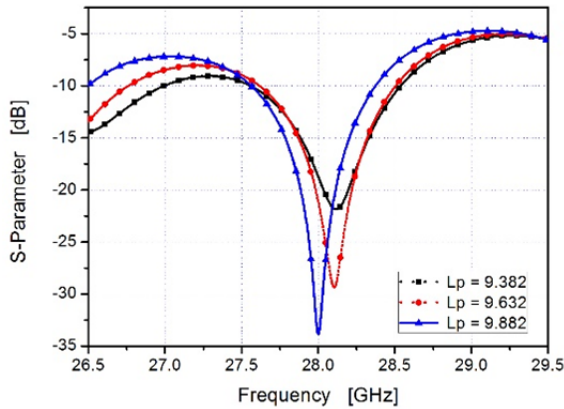


Fig. 7. A parametric study of increasing the length  $L_p$ .

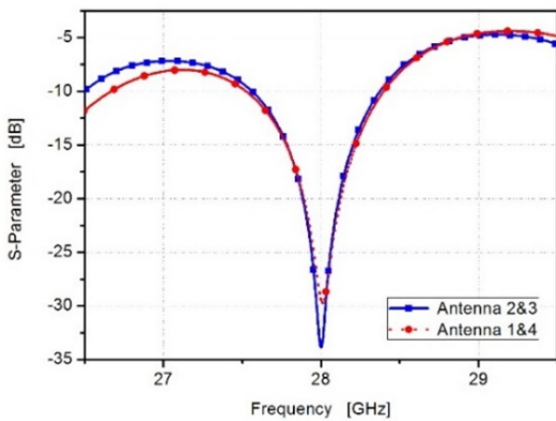


Fig. 8. The return loss of the complete antenna structure, blue curve for antenna 2&3 and the red one for antenna 1&4.

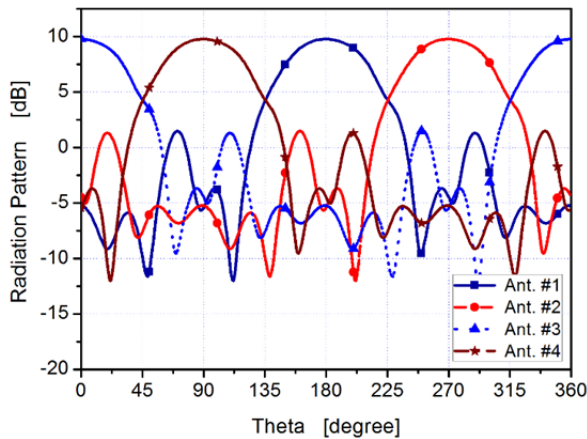


Fig. 9. The radiation pattern of the complete antenna structure.

### 3. Results and Discussion

#### 3.1 Single Element

The proposed single element Vivaldi antenna is designed and simulated by CST software. This structure is operated at a resonance frequency of 28 GHz to cover the ITS and 5G applications. It has a return loss of 31.5 dB at a resonance frequency. The antenna is fabricated using the photolithography method and measured using vector network analyzer (R&S ZVA 67). Figure 10 shows the fabricated single element antenna. Good agreement is achieved between the simulated and measured results



Fig. 10. The fabricated antenna design.

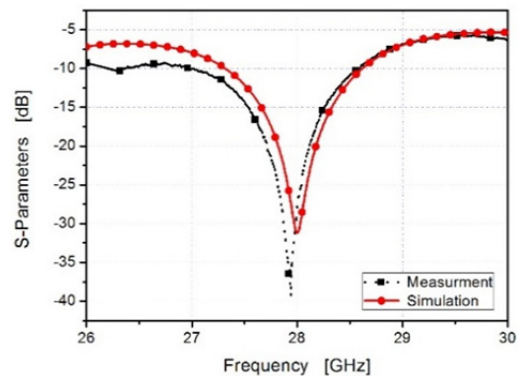


Fig. 11. The comparison of simulated and measured  $S_{11}$  results for a single element antenna.

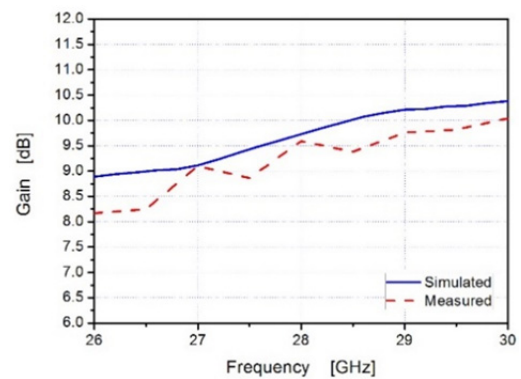


Fig. 12. The comparison between simulated and measured overall gain versus frequency results for the single element.

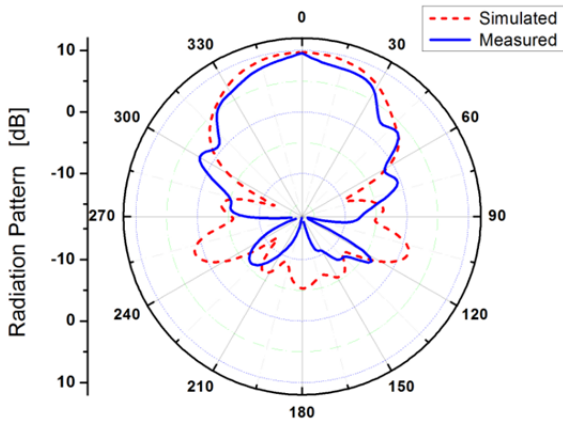


Fig. 13. The comparison between simulated and measured radiation pattern.

The return loss comparison curves are shown in Fig. 11. The gain of the antenna is also measured and Figure 12 shows the comparison between measured and simulated results. The comparison between simulated and measured radiation pattern (normalized) is introduced as shown in Fig. 13.

### 3.2 Complete Structure

The complete antenna structure is designed on same substrate of “Rogers 5880”. The complete antenna structure is fabricated and measured. Figure 14 shows the fabricated antenna structure. The return loss is measured and compared with the simulated. Figure 15 shows the return loss

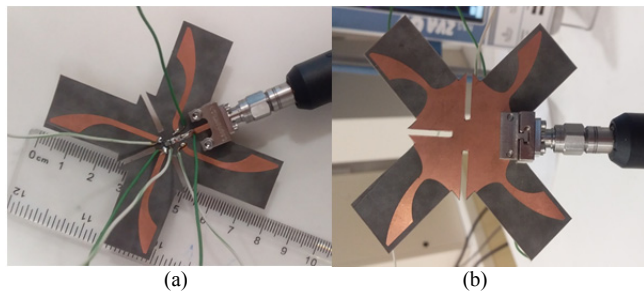


Fig. 14. The fabricated antenna structure (a) top view, and (b) bottom view.

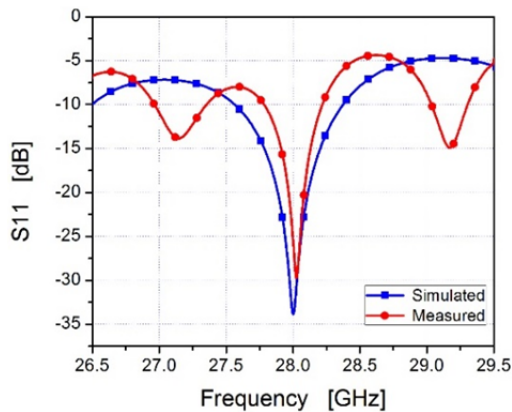


Fig. 15. The comparison of simulated and measured  $S_{11}$  results for antenna 1 & 4 in the complete structure.

for antenna 1&4 elements. The measured result is close to the simulated one with some notches. Figure 16 shows the return loss for antenna 2&3 elements. The radiation pattern

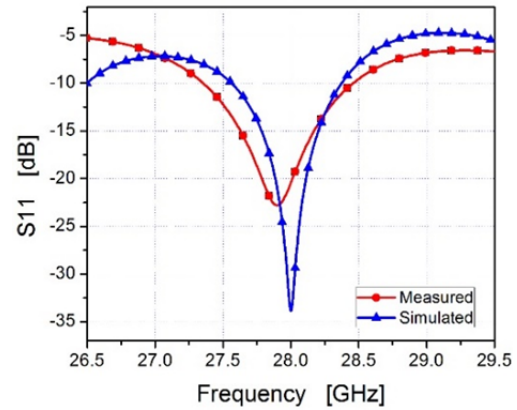
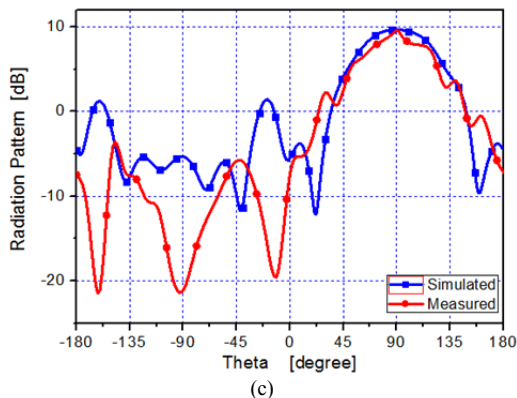
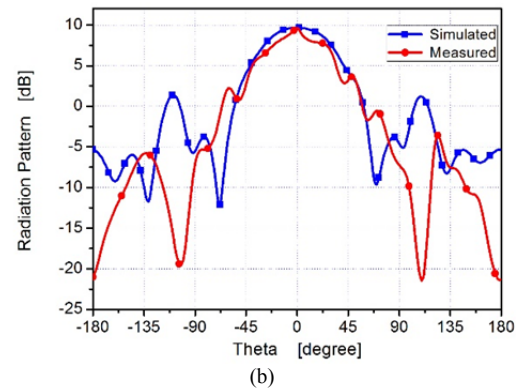
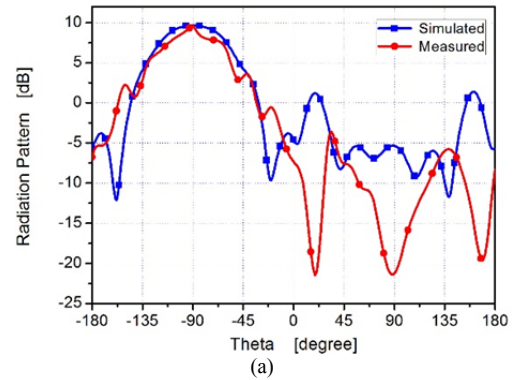


Fig. 16. The comparison of simulated and measured  $S_{11}$  results for antenna 2 & 3 in the complete structure.



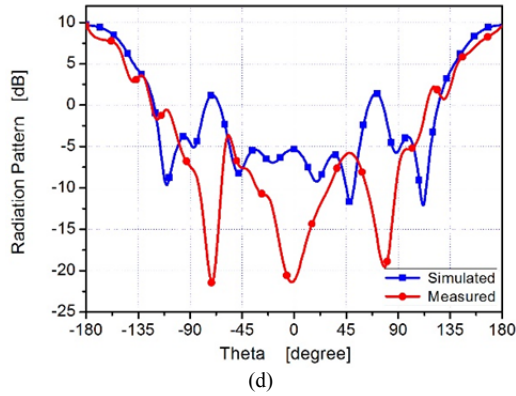


Fig. 17. The comparison between simulation and measurements of overall structure radiation pattern.

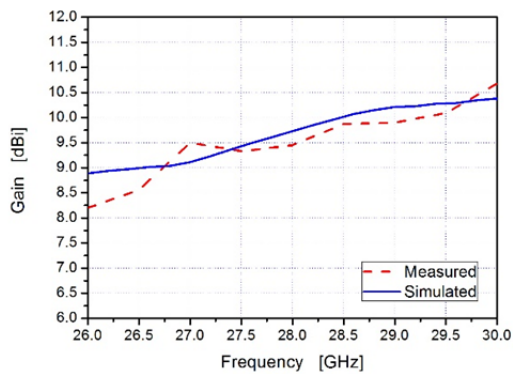


Fig. 18. The comparison between simulated and measured overall gain versus frequency results for a single element within the complete structure.

Paper	[10]	[15]	[20]	[21]	[22]	This work
Center frequency [GHz]	0.6, 7	60	26	6	28	28
Bandwidth (at -10 dB) [%]	14.3	3.33	10.58	33.3	14.3	5.86
Coverage area [degree]	360	90	Narrow	360	54	360
Gain [dBi]	5.8	3	12.9	7.7	12.8	9.78
Size [in mm]	144 ×144	14.7 ×11.9	54.4 ×28.2	80 ×80	34 ×55.8	48.85 ×48.85

Tab. 4. Comparison with pervious works.

and the gain are also measured and compared with the simulated. Good agreements are achieved between the simulated and measured results. Figure 17 shows the comparison between the simulated and measured radiation pattern. Figure 18 shows the overall gain versus frequency for the complete structure. The comparison between this work and previous works is tabulated in Tab. 4.

### 4. Conclusion

A 28 GHz switched beam Vivaldi antenna system consists of 4 elements of Vivaldi antennas for V2V com-

munication in 5G application is introduced. The designed antenna achieves wide bandwidth of 5.38% around the operating center frequency of 28 GHz. The omnidirectional radiation is achieved by using 4-elements of Vivaldi antennas. The antenna shows remarkable radiation characteristics and high-gain of more than 9.78 dBi. The proposed antenna achieves a bandwidth of 1.64 GHz for the single element and 1.11 GHz for the complete structure. The antenna is fabricated and measured.

### References

- [1] CHOWDHURY, M., DEY, K. C. Intelligent transportation systems-a frontier for breaking boundaries of traditional academic engineering disciplines. *IEEE Intelligent Transportation Systems Magazine*, 2016, vol. 8, no. 1, p. 4–8. DOI: 10.1109/MITS.2015.2503199
- [2] ZHONG, Z. P., ZHANG, X., LIANG, J. J., et al. A compact dual-band circularly polarized antenna with wide axial-ratio beamwidth for vehicle GPS satellite navigation application. *IEEE Transactions on Vehicular Technology*, 2019, vol. 68, no. 9, p. 8683–8692. DOI: 10.1109/TVT.2019.2920520
- [3] VIRIYASITAVAT, W., BOBAN, M., TSAI, H. M., et al. Vehicular communications: Survey and challenges of channel and propagation models. *IEEE Vehicular Technology Magazine*, 2015, vol. 10, no. 2, p. 55–66. DOI: 10.1109/MVT.2015.2410341
- [4] WEN, L., GAO, S., LUO, Q., et al. Wideband dual circularly polarized antenna for intelligent transport systems. *IEEE Transactions on Vehicular Technology*, 2020, vol. 69, no. 5, p. 5193–5202. DOI: 10.1109/TVT.2020.2980382
- [5] JILANI, S. F., ALOMAINY, A. A multiband millimeter-wave 2-D array based on enhanced Franklin antenna for 5G wireless systems. *IEEE Antennas and Wireless Propagation Letters*, 2017, vol. 16, no. 9, p. 2983–2986. DOI: 10.1109/LAWP.2017.2756560
- [6] LI, C., CHEN, W., YU, J., et al. V2V radio channel properties at urban intersection and ramp on urban viaduct at 5.9 GHz. *IET Communications*, 2018, vol. 12, no. 17, p. 2198–2205. DOI: 10.1049/iet-com.2018.5247
- [7] WEVERS, K., LU, M. V2X communication for ITS-from IEEE 802.11p towards 5G. *IEEE 5G Tech Focus*, June 2017, vol. 1, no. 2.
- [8] LIU, A., LU, Y., HUANG, L. Low-profile patch antennas with enhanced horizontal omnidirectional gain for DSRC applications. *IET Microwaves, Antennas and Propagation*, 2018, vol. 12, no. 2, p. 246–253. DOI: 10.1049/iet-map.2017.0845
- [9] NGUYEN-TRONG, N., PINAPATI, S. P., HALL, D., et al. Ultralow-profile and flush-mounted monopolar antennas integrated into a metallic cavity. *IEEE Antennas and Wireless Propagation Letters*, 2018, vol. 17, no. 1, p. 86–89. DOI: 10.1109/LAWP.2017.2776290
- [10] LEE, M. W., JEONG, N. S. Low-profile vehicle roof-top mounted broadband antenna for V2X. In *IEEE International Symposium on Antennas and Propagation and USNC-URSI Radio Science Meeting*. Atlanta (GA, USA), 2019, p. 925–926. DOI: 10.1109/APUSNCURSINRSM.2019.8889343
- [11] ARTNER, G., LANGWIESER, R., MECKLENBRÄUKER, C. F. Concealed CFRP vehicle chassis antenna cavity. *IEEE Antennas and Wireless Propagation Letters*, 2017, vol. 16, p. 1415–1418. DOI: 10.1109/LAWP.2016.2637560
- [12] NGUYEN-TRONG, N., PIOTROWSKI, A., KAUFMANN, T., et al. Low-profile wideband monopolar UHF antennas for integration onto vehicles and helmets. *IEEE Transactions on Antennas and*

- Propagation*, 2016, vol. 64, no. 6, p. 2562–2568. DOI: 10.1109/TAP.2016.2551291
- [13] SEMKIN, V., FERRERO, F., BISOGNIN, A., et al. Beam switching conformal antenna array for mm-wave communications. *IEEE Antennas and Wireless Propagation Letters*, 2015, vol. 15, p. 28–31. DOI: 10.1109/LAWP.2015.2426510
- [14] DARVAZEHBAN, A., REZAEIEH, S. A., ABBOSH, A. Wideband beam-switched bow-tie antenna with inductive reflector. *IEEE Antennas and Wireless Propagation Letters*, 2020, vol. 19, no. 10, p. 1724–1728. DOI: 10.1109/LAWP.2020.3015512
- [15] TRZEBIATOWSKI, K., RZYMOWSKI, M., KULAS, L., et al. Simple 60 GHz switched beam antenna for 5G millimeter-wave applications. *IEEE Antennas and Wireless Propagation Letters*, 2021, vol. 20, no. 1, p. 38–42. DOI: 10.1109/LAWP.2020.3038260
- [16] VENKATESWARAN, V., PIVIT, F., GUAN, L. Hybrid RF and digital beamformer for cellular networks: Algorithms, microwave architectures, and measurements. *IEEE Transactions on Microwave Theory and Techniques*, 2016, vol. 64, no. 7, p. 2226–2243. DOI: 10.1109/TMTT.2016.2569583
- [17] BANTAVIS, P. I., KOLITSIDAS, C. I., EMPLIOUK, T., et al. A cost-effective wideband switched beam antenna system for a small cell base station. *IEEE Transactions on Antennas and Propagation*, 2018, vol. 66, no. 12, p. 6851–6861. DOI: 10.1109/TAP.2018.2874494
- [18] SARKIS, R., CRAEYE, C. Circular array of wideband 3D Vivaldi antennas. In *URSI International Symposium on Electromagnetic Theory*. Berlin (Germany), 2010, p. 792–794. DOI: 10.1109/URSI-EMTS.2010.5637231
- [19] RMILI, H., ALKHALIFEH, K., ZAROUAN, M., et al. Numerical analysis of the microwave treatment of palm trees infested with the red palm weevil pest by using a circular array of Vivaldi antennas. *IEEE Access*, 2020, vol. 8, p. 152342–152350. DOI: 10.1109/ACCESS.2020.3017517
- [20] LIU, H., YANG, W., ZHANG, A., et al. A miniaturized gain-enhanced antipodal Vivaldi antenna and its array for 5G communication applications. *IEEE Access*, 2018, vol. 6, p. 76282–76288. DOI: 10.1109/ACCESS.2018.2882914
- [21] DENG, C., CHEN, W., ZHANG, Z., et al. Generation of OAM radio waves using circular Vivaldi antenna array. *International Journal of Antennas and Propagation*, 2013, p. 1–7. DOI: 10.1155/2013/847859
- [22] ELABD, R. H., ABDULLAH, H. H., ABDELAZIM, M. Compact highly directive MIMO Vivaldi antenna for 5G millimeter-wave base station. *Journal of Infrared, Millimeter, and Terahertz Waves*, 2021, vol. 42, no. 2, p. 173–194. DOI: 10.1007/s10762-020-00765-4
- [23] DU, Y. X., LIU, H., QIN, L., et al. Integrated multimode orbital angular momentum antenna based on RF switch. *IEEE Access*, 2020, vol. 8, p. 48599–48606. DOI: 10.1109/ACCESS.2020.2979945
- [24] DARVAZEHBAN, A., REZAEIEH, S. A., MANOOCHEHRI, O., et al. Two-dimensional pattern-reconfigurable cross-slot antenna with inductive reflector for electromagnetic torso imaging. *IEEE Transactions on Antennas and Propagation*, 2020, vol. 68, no. 2, p. 703–711. DOI: 10.1109/TAP.2019.2940617
- [25] REZAEIEH, S. A., ZAMANI, A., ABBOSH, A. M. Pattern reconfigurable wideband loop antenna for thorax imaging. *IEEE Transactions on Antennas and Propagation*, 2019, vol. 67, no. 8, p. 5104–5114. DOI: 10.1109/TAP.2018.2889164
- [26] CHOU, H. T., CHANG, Y. S., HUANG, H. J., et al. Two-dimensional multi-ring dielectric lens antenna to radiate fan-shaped multi-beams with optimum adjacent-beam overlapping crossover by genetic algorithm. *IEEE Access*, 2020, vol. 8, p. 79124–79133. DOI: 10.1109/ACCESS.2020.2990223